

Numerical Simulation of Bilaminates with Periodic Hyperelastic Phases

A. R. Aguiar

Department of Structural Engineering
São Carlos School of Engineering, University of São Paulo
aguiarar@sc.usp.br

E. B. T. Prado

Department of Structural Engineering
São Carlos School of Engineering, University of São Paulo
edmarbt@sc.usp.br

...

ABSTRACT

Phenomena like strain localization in hyperelastic materials are intrinsically nonlinear and are related to the loss of ellipticity of the Hessian of the strain energy function. Solutions of the associated nonlinear problems are usually not known. Analytical methods, such as homogenization methods, and numerical methods, such as the Finite Element Method, are used to search for approximate solutions to these problems, which may lose ellipticity at large enough deformations. In this case, an approximate solution may not correspond to a stable and, therefore, realistic solution of the nonlinear problem. Other solutions that are stable may bifurcate from this approximate solution. The class of problems considered in this work involves bilaminates with distinct hyperelastic phases that alternate periodically. The materials of these phases are such that no stability issues are expected to occur. The bilaminates are in equilibrium and are subjected to prescribed deformations on their boundaries. A tangent second-order homogenization method is used in the literature to gain insight on the effective behavior of the hyperelastic laminates. Solutions of the corresponding homogenized problems, called principal solutions, are found and a stability analysis is performed, which shows that the principal solutions may bifurcate into stable solutions at sufficiently large deformations. These results seem to indicate that the overall behavior of a laminate may be unstable even when the behavior of each underlying constituent is not. In this work, we simulate numerically the behavior of bilaminates in the above class by imposing the same boundary conditions used elsewhere in the literature. By comparing principal and approximate numerical solutions, we find that both solutions are indistinguishable for small deformations and are quite different for large deformations. The implications of these results are still under investigation. This research finds applications in various fields of engineering, which include the development of new materials with lamellar microstructure.

Keywords: Nonlinear Elasticity; Hyperelastic Laminate; Computational Mechanics; Material Instability.

1 INTRODUCTION

In [1] the problem of a bilaminate in equilibrium without body force subjected to prescribed deformation on its boundary is considered. The bilaminate is composed of distinct hyperelastic phases that alternate periodically. The authors use a second-order homogenization method developed by [2] to obtain a *principal solution* to this problem and investigate the onset of macroscopic instabilities by analyzing the loss of strong ellipticity of an effective stored energy function of the bilaminate evaluated at the principal solution.

In this paper we consider a bilaminate in equilibrium in the absence of body force subject to both a state of plane strain and pure shear imposed on its boundary. Although the procedure of analysis is general, we restrict our attention to the compressible Neo-Hookean material model that is implemented in the finite element package ANSYS 10.0¹. We use the theoretical framework presented by [1] and authors cited therein to obtain analytical results for the effective medium. In particular, we obtain a principal solution that renders the system of governing differential equations non-elliptic for a large enough deformation prescribed on the boundary. Our analytical results are analogous to analytical results obtained by [1] in the analysis of a bilaminate made of a different compressible Neo-Hookean material. We then use the finite element package ANSYS 10.0 to find an approximate solution to the bilaminate problem. The numerical results obtained from this solution are in very good agreement with the analytical results for small deformations and are quite different for large deformations, indicating that the solution found via ANSYS may be an approximation of a *secondary solution* that bifurcates from the principal solution.

In Section 2 we present some preliminaries about kinematics of large deformation, governing equilibrium equations, and formulation of the boundary value problem of interest in this work. In Section 3 we define the bilaminate and, using the tangent second-order homogenization method, present some expressions that represent its macroscopic behavior. In Section 4 we introduce the compressible Neo-Hookean material model implemented in ANSYS 10.0, present the analytical expression for the average deformation gradient of the effective medium, and use this expression to obtain the angle of lamination of the bilaminate in its deformed configuration. In the final part of Section 4 we present graphs for the angle of lamination of the bilaminate in its deformed configuration that were obtained from both the analytical expression and computational results from ANSYS 10.0. In Section 5 we present some concluding remarks.

2 PRELIMINARIES

Let $\mathcal{B} \subset \mathbb{R}^3$ be the undistorted reference configuration of a body and let $\mathbf{x} : \mathcal{B} \rightarrow \mathbb{R}^3$ be a deformation field acting on the body. We have that $\mathbf{x}(\mathbf{X})$ is the position of the particle $\mathbf{X} \in \mathcal{B}$ relative to a fixed frame \mathbf{F} in \mathbb{R}^3 . The displacement field associated with the deformation \mathbf{x} is defined by $\mathbf{u}(\mathbf{X}) = \mathbf{x}(\mathbf{X}) - \mathbf{X}$. In a rectangular Cartesian coordinate system fixed at the origin, we write X_i , x_i , and u_i for the components of these vector fields. The deformation gradient is then given by

$$\mathbf{F} \equiv \text{grad } \mathbf{x} = \mathbf{1} + \text{grad } \mathbf{u}, \quad F_{ij} = \frac{\partial x_i}{\partial X_j} = \delta_{ij} + \frac{\partial u_i}{\partial X_j}, \quad i, j = 1, 2, 3, \quad (1)$$

where $\text{grad} : \mathbb{R}^3 \rightarrow \mathcal{L}$ is the gradient operator for vector fields, with \mathcal{L} being the set of second-order tensors, $\mathbf{1}$ is the identity tensor, and F_{ij} and δ_{ij} are the components of \mathbf{F} and $\mathbf{1}$, respectively.

The body is in equilibrium in the absence of body force, which means that

$$\text{div } \mathbf{P} = \mathbf{0}, \quad \frac{\partial P_{ij}}{\partial X_j} = 0 \quad \text{in } \mathcal{B}, \quad i = 1, 2, 3, \quad (2)$$

where $\text{div} : \mathcal{L} \rightarrow \mathbb{R}^3$ is the divergence operator for tensor fields, $\mathbf{P} : \mathcal{B} \rightarrow \mathcal{L}$ is the first Piola-Kirchhoff stress tensor, P_{ij} are the components of \mathbf{P} , and the usual summation convention over

¹ ANSYS 10.0 is a software of *Ansys Inc.*, PA, USA.

repeated indices is used throughout this work.

The body is *hyperelastic* and *heterogeneous*, so that \mathbf{P} is the derivative of a stored strain energy density function $W : \mathcal{L} \times \mathcal{B} \rightarrow \mathbb{R}$ at \mathbf{F} for a material point $\mathbf{X} \in \mathcal{B}$, that is,

$$\mathbf{P} = DW(\mathbf{F}, \mathbf{X}), \quad P_{ij} = \frac{\partial W(\mathbf{F}, \mathbf{X})}{\partial F_{ij}}, \quad \mathbf{F} \in \mathcal{L}, \quad \mathbf{X} \in \mathcal{B}, \quad i, j = 1, 2, 3. \quad (3)$$

If $DW(\mathbf{F}, \cdot)$ does not depend explicitly on $\mathbf{X} \in \mathcal{B}$, then the body is *homogeneous* and we write $\mathbf{P} = DW(\mathbf{F})$.

If $W(\mathbf{F}, \mathbf{X})$ is smooth with respect to its arguments in a given part \mathcal{P} of \mathcal{B} , we can substitute (3) into the equilibrium equation (2) and use the chain rule to get

$$\frac{\partial^2 W(\mathbf{F}, \mathbf{X})}{\partial F_{ij} \partial F_{kl}} \frac{\partial^2 x_k}{\partial X_j \partial X_l} + \frac{\partial^2 W(\mathbf{F}, \mathbf{X})}{\partial X_j \partial F_{ij}} = 0, \quad \mathbf{F} \in \mathcal{L}, \quad \mathbf{X} \in \mathcal{P} \subset \mathcal{B}, \quad i = 1, 2, 3, \quad (4)$$

where the second derivatives $\partial^2 W / \partial F_{ij} \partial F_{kl}$ are the components of the elasticity tensor $\mathbb{A}(\mathbf{F}, \mathbf{X}) \equiv D^2 W(\mathbf{F}, \mathbf{X})$, which is a fourth-order tensor evaluated at \mathbf{F} for the material point $\mathbf{X} \in \mathcal{P}$. This tensor plays an important role in the investigation of new phenomena in solid mechanics. For instance, consider the *Legendre-Hadamard condition*

$$(\mathbf{b} \otimes \mathbf{c}) : \mathbb{A}[\mathbf{b} \otimes \mathbf{c}] > 0, \quad \mathbf{b}, \mathbf{c} \in \mathbb{R}^3, \quad (5)$$

where “:” denotes the inner product in \mathcal{L} and $\mathbb{A}[\mathbf{G}] \in \mathcal{L}$ for $\mathbf{G} \in \mathcal{L}$, with components $A_{ijkl} G_{kl}$. Also known as the *strong ellipticity condition*, it substantiates the experimental evidence according to which *a body is elongated in the direction of the applied forces* ([3] APUD [4]). On the other hand, the violation of this condition is associated with the formation of shear bands, which may lead to material failure by localization of shear deformation ([5,6]). In Classical Linear Elasticity, $\mathbb{C}(\mathbf{X})[\mathbf{E}] \equiv \mathbb{A}(\mathbf{1}, \mathbf{X})[\mathbf{E}] = \lambda(\mathbf{X})(\mathbf{E} : \mathbf{1})\mathbf{1} + 2\mu(\mathbf{X})\mathbf{E}$, where $\mathbf{E} \in \mathcal{L}$ is symmetric and both λ and μ are the Lamé moduli. Here, the condition (5) is equivalent to having both $\mu > 0$ and $\lambda + 2\mu > 0$.

We shall consider displacement boundary conditions of the form

$$\mathbf{u} = \bar{\mathbf{u}}, \quad \mathbf{X} \in \partial\mathcal{B}, \quad (6)$$

where $\bar{\mathbf{u}} : \partial\mathcal{B} \rightarrow \mathbb{R}^3$ is a known displacement field imposed on the boundary of \mathcal{B} . A well-known particular case of (6) corresponds to $\bar{\mathbf{u}} = (\bar{\mathbf{F}} - \mathbf{1})\mathbf{X}$, where $\bar{\mathbf{F}} \in \mathcal{L}$ is constant. We then have that a boundary value problem of elastostatics in this work consists of finding the deformation field $\mathbf{x} = \mathbf{u} + \mathbf{X} : \mathcal{B} \rightarrow \mathbb{R}^3$ that satisfies the equilibrium equations (4), where \mathbf{F} is given by (1), together with a displacement boundary condition of the form (6).

3 EFFECTIVE PROPERTIES OF NONLINEAR LAMINATES

We consider a laminate obtained from a periodic distribution of cells in the X_1 – direction, where each cell is composed of two consecutive plane laminae of same width W , same height H , and lengths L_1 and L_2 in a reference configuration of the body, as illustrated in Fig. 1. We then have that the reference configurations of the laminate and its periodicity cell are given by $\mathcal{B} = \mathcal{B}_1 \cup \mathcal{B}_2$, $\mathcal{B}_1 \cap \mathcal{B}_2 = \emptyset$, and $\Omega \equiv \Omega_1 \cup \Omega_2$, $\Omega_1 \cap \Omega_2 = \emptyset$, respectively, where \mathcal{B}_r and

Ω_r , $r=1,2$, are the undistorted reference configurations of the phase r of the laminate and its periodicity cell, respectively.

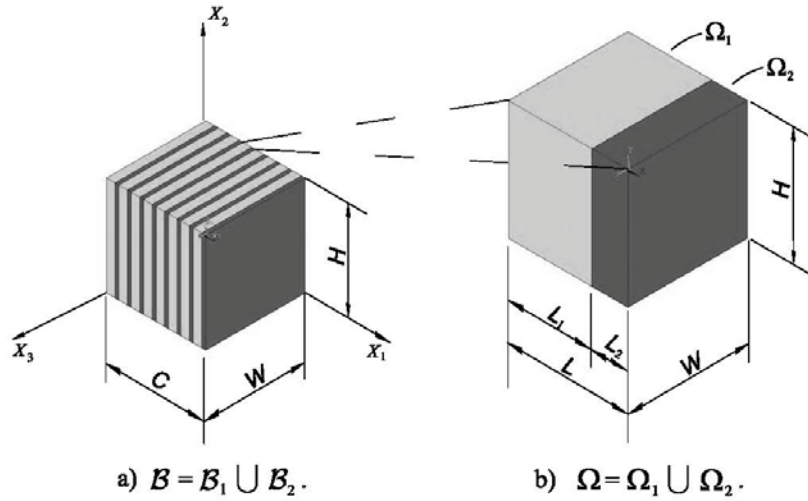


Figure 1: Reference configurations of **a)** Laminate; **b)** Periodicity cell of the laminate.

Phase r is isotropic and hyperelastic, with strain energy function $W_r : \mathcal{L} \rightarrow \mathbb{R}$. Using the characteristic function $\chi_r : \mathcal{B} \rightarrow \{0,1\}$ to identify the undistorted configuration of phase r in \mathcal{B} , we can write the strain energy function $W : \mathcal{L} \times \mathcal{B} \rightarrow \mathbb{R}$ that appears in (3) as a piecewise continuous function given by

$$W(\mathbf{F}, \mathbf{X}) = W_r(\mathbf{F}) \chi_r(\mathbf{X}), \quad \mathbf{F} \in \mathcal{L}, \quad \mathbf{X} \in \mathcal{B}. \quad (7)$$

Substituting (7) into (3), we obtain the mechanical response of the material in an arbitrary point $\mathbf{X} \in \mathcal{B}$. This response is local, or, microscopic and depends upon the knowledge of the associated deformation field, which is, in general, evaluated approximately using numerical methods. In [7] we use a Finite Element Method (FEM) to obtain approximate solutions of uni-axial tension problems involving linearly elastic bilaminates. We also use an Asymptotic Homogenization Method to obtain a global, or, macroscopic response of the laminate, which coincides with the response function obtained from the numerical results when both the number of laminae in a laminate with fixed dimensions and the number of degrees of freedom in the numerical approximation tends to infinity.

In the nonlinear case, analogous results are still the subject of intense investigation (see, for instance, [1,8]) due not only to the complexity of the analysis of the associated nonlinear problems, but also to the possibility of material instabilities that can generate multiple solutions for a given problem.

A procedure of analysis consists of assuming that a global, or, macroscopic relation for the laminate is given by (see, for instance, [9])

$$\bar{\mathbf{P}} = D\bar{W}(\bar{\mathbf{F}}), \quad (8)$$

where $\bar{\mathbf{P}} \equiv \langle \mathbf{P} \rangle$, $\bar{\mathbf{F}} \equiv \langle \mathbf{F} \rangle$, with $\langle \cdot \rangle \equiv \int_{\mathcal{B}} (\cdot) d\mathbf{Y} / |\mathcal{B}|$ and $|\mathcal{B}|$ being the volume of \mathcal{B} , and

$$\bar{W}(\bar{\mathbf{F}}) \equiv \min_{\mathbf{F} \in \mathcal{K}(\bar{\mathbf{F}})} \langle W(\mathbf{F}, \mathbf{X}) \rangle = \sum_{r=1}^2 \min_{\mathbf{F} \in \mathcal{K}(\bar{\mathbf{F}})} c_r \langle W_r(\mathbf{F}) \rangle_r, \quad c_r \equiv \frac{L_r}{L}, \quad (9)$$

is the strain energy function of the resulting homogenized medium. In (9),

$$\mathcal{K}(\bar{\mathbf{F}}) \equiv \left\{ \mathbf{F} \mid \exists \hat{\mathbf{X}} = \mathbf{x}(\mathbf{X}) \text{ with } \mathbf{F}(\mathbf{X}) \equiv \text{grad } \mathbf{x}(\mathbf{X}) \text{ in } \mathcal{B}, \hat{\mathbf{X}} = \bar{\mathbf{F}} \mathbf{X} \text{ on } \partial \mathcal{B} \right\} \quad (10)$$

is the set of kinematically admissible deformation gradients and $\langle \cdot \rangle_r \equiv \int_{\mathcal{B}_r} (\cdot) d\mathbf{Y} / |\mathcal{B}_r|$, $r=1,2$, where $|\mathcal{B}_r|$ is the volume of the r th lamina in the reference configuration \mathcal{B}_r . Also, c_r , $r=1,2$, is the volume fraction of phase r in the reference configuration of the laminate.

The next step in this procedure is to formulate the associated boundary value problem of elastostatics, which consists of finding the deformation field $\bar{\mathbf{x}}: \mathcal{B} \rightarrow \mathbb{R}^3$, with corresponding deformation gradient $\mathbf{F} = \text{grad } \mathbf{x}$ belonging to the set $\mathcal{K}(\bar{\mathbf{F}})$, that satisfies the equilibrium equations (4) with W replaced by \bar{W} , with no explicit dependence on $\mathbf{X} \in \mathcal{B}$, and \mathbf{F} replaced by $\bar{\mathbf{F}}$. Assuming homogeneous deformations in the different laminae and imposing continuity of both traction and deformation at the lamina interfaces, we obtain an equilibrium solution, called principal solution, of the boundary value problem. Bifurcations may occur from this solution due to material instability associated to the loss of ellipticity of the equilibrium equations. In this case, stable secondary solutions, which are physically meaningful, may co-exist with principal solutions, which become unstable and, therefore, impossible to occur in the “real world”.

In [1] the onset of macroscopic instabilities investigated by analyzing the loss of strong ellipticity of an effective strain energy function of the bilaminate evaluated at a principal solution. Using a second-order homogenization method developed by [2], it is shown in [1] that the effective strain energy function may be written in the form

$$\hat{W}(\bar{\mathbf{F}}) = c_1 W_1(\bar{\mathbf{F}}_1) + c_2 W_2(\bar{\mathbf{F}}_2), \quad (11)$$

where both $\bar{\mathbf{F}}_r \equiv \langle \mathbf{F} \rangle_r$, $r=1,2$, must satisfy the global average condition

$$\bar{\mathbf{F}} = c_1 \bar{\mathbf{F}}_1 + c_2 \bar{\mathbf{F}}_2 \quad (12)$$

and we recall from above that $W_r: \mathcal{L} \rightarrow \mathbb{R}$, $r=1,2$, is the strain energy function of phase r , which is isotropic and homogeneous. The authors also show that

$$D^2 \hat{W}(\bar{\mathbf{F}}) = D^2 W_1(\bar{\mathbf{F}}_1) + c_2 \left[c_1 \mathbf{H} - \left(D^2 W_1(\bar{\mathbf{F}}_1) - D^2 W_2(\bar{\mathbf{F}}_2) \right)^{-1} \right], \quad (13)$$

where the components of the fourth-order tensor \mathbf{H} are given by

$$H_{ijkl} \equiv (\mathbf{K}^{-1})_{ik} N_j N_l, \quad K_{ik} \equiv \left(D^2 W_1(\bar{\mathbf{F}}_1) \right)_{ipkq} N_p N_q, \quad (14)$$

with N_p , $p=1,2,3$, being the components of the direction \mathbf{N} of lamination of the bilaminate in its reference configuration. In this work, $\mathbf{N} = \mathbf{e}_1$.

Replacing $\mathbb{A}(\mathbf{F}, \mathbf{X})$ in the strong ellipticity condition (5) by $D^2 \hat{W}(\bar{\mathbf{F}})$, the authors argue that macroscopic instability may occur in the corresponding effective medium whenever the resulting strong ellipticity condition is violated for some $\bar{\mathbf{F}}$. It is clear from (9) and (11) that $\bar{W}(\bar{\mathbf{F}}) = \hat{W}(\bar{\mathbf{F}})$ from the reference configuration, $\bar{\mathbf{F}} = \mathbf{1}$, up to the onset of the first instability, after which $\bar{W}(\bar{\mathbf{F}}) \leq \hat{W}(\bar{\mathbf{F}})$.

The previous assumption concerning homogeneous deformation in each lamina is reasonable away from the boundary of a finite laminate, or, in the interior of laminates with infinite dimensions. In the next section we consider a special class of hyperelastic materials together with a particular expression for $\bar{\mathbf{F}}$ in (10) and concentrate on the analysis of the angles of lamination of

bilaminates in their deformed configurations using both the theory outlined above and computational results obtained from finite element solutions of boundary value problems defined for laminates with finite dimensions. To obtain the angles of lamination in this last case, we consider that the deformations of consecutive laminae at the centers of the bilaminates are approximately homogeneous. This has been verified numerically.

4 NUMERICAL RESULTS

Recall from Section 3 that we consider a two-phase laminate composed of periodically alternating homogeneous laminae along the X_1 -direction. The laminae are perfectly bonded to each other and the reference configuration of the periodicity cell is given by $\Omega = \Omega_1 \cup \Omega_2$, as illustrated in Fig. 1.b. We also consider a fixed orthonormal basis $\{\mathbf{e}_1, \mathbf{e}_2, \mathbf{e}_3\}$ for the rectangular Cartesian coordinate system.

Recall from (11) and (12) that the principal solution for the boundary value problem of the effective medium is piecewise homogeneous. Here, we investigate numerically the possibility of a secondary solution to exist. For this, we consider strain energy functions of compressible Neo-Hookean materials for the hyperelastic phases given by

$$W_1(\mathbf{F}) = \frac{\mu_1}{2} \left(\frac{\mathbf{F} : \mathbf{F}}{(\det \mathbf{F})^{2/3}} - 3 \right) + \frac{\kappa_1}{2} (\det \mathbf{F} - 1)^2, \quad W_2(\mathbf{F}) = \tau W_1(\mathbf{F}), \quad (15)$$

where μ_r and κ_r , $r = 1, 2$, denote the shear and volumetric elasticity moduli, respectively, in the reference configuration of the hyperelastic body and the factor $\tau \in \mathbb{R}$ quantifies the heterogeneity contrast between phases 1 and 2. These material models are implemented in the finite element commercial package ANSYS 10.0.

Incidentally, in [1] different strain energy density functions of compressible Neo-Hookean materials for the hyperelastic phases are used, being given by

$$W_1(\mathbf{F}) = \frac{\mu_1}{2} \left[\mathbf{F} : \mathbf{F} - 3 - \log(\det \mathbf{F})^2 \right] + \left(\frac{\kappa_1}{2} - \frac{\mu_1}{3} \right) (\det \mathbf{F} - 1)^2, \quad W_2(\mathbf{F}) = \tau W_1(\mathbf{F}), \quad (16)$$

where μ_r and κ_r , $r = 1, 2$, and $\tau \in \mathbb{R}$ denote the same material constants introduced in (15). It is not difficult to show that the strong ellipticity condition (5) is satisfied in each phase modeled by (16) for the values of μ_r and κ_r , $r = 1, 2$, considered below. In the case of (15), we have verified numerically that the condition (5) is also satisfied in each phase for the same values of μ_r and κ_r , $r = 1, 2$. Both (15) and (16) yield the (incompressible) Neo-Hookean material in the limit of incompressibility, $\det \mathbf{F} = 1$.

Substituting (15) into (7) and then substituting the resulting expression into (3), we obtain

$$\mathbf{P} \equiv \tilde{\mathbf{P}}(\mathbf{F}, \mathbf{X}) = \chi_r(\mathbf{X}) \operatorname{cof} \mathbf{F} \left[\frac{\mu_r}{(\det \mathbf{F})^{5/3}} \left(\mathbf{C} - \frac{I_1}{3} \mathbf{1} \right) + \kappa_r (\det \mathbf{F} - 1) \mathbf{1} \right], \quad (17)$$

where $\chi_r : \mathcal{B} \rightarrow \{0, 1\}$ is the characteristic function introduced in Section 3.

We consider the same boundary conditions used by [1] in their analysis. We assume a state of

plane strain parallel to the unit vectors $\{\mathbf{e}_1, \mathbf{e}_2\}$ and consider that, relative to the orthonormal basis $\{\mathbf{e}_1, \mathbf{e}_2, \mathbf{e}_3\}$, the matrix representation of $\bar{\mathbf{F}}$ in (10) is given by

$$[\bar{\mathbf{F}}] = \begin{pmatrix} \cos \bar{\Theta} & -\sin \bar{\Theta} & 0 \\ \sin \bar{\Theta} & \cos \bar{\Theta} & 0 \\ 0 & 0 & 1 \end{pmatrix} \begin{pmatrix} \bar{\lambda} & 0 & 0 \\ 0 & \bar{\lambda}^{-1} & 0 \\ 0 & 0 & 1 \end{pmatrix} \begin{pmatrix} \cos \bar{\Theta} & \sin \bar{\Theta} & 0 \\ -\sin \bar{\Theta} & \cos \bar{\Theta} & 0 \\ 0 & 0 & 1 \end{pmatrix}, \quad (18)$$

where $\bar{\lambda}^2 \geq 1$ and $\bar{\lambda}^{-2}$ are the principal stretches of $\bar{\mathbf{C}} \equiv \bar{\mathbf{F}}^T \bar{\mathbf{F}}$ in the plane defined by the unit vectors $\{\mathbf{e}_1, \mathbf{e}_2\}$ and $\bar{\Theta} \in [0, \pi/2]$ yields the orientation, in the anti-clockwise direction from the \mathbf{e}_1 -direction, of the principal axes of $\bar{\mathbf{C}}$. The homogeneous deformation obtained from $\bar{\mathbf{F}}$ corresponds to a state of pure shear. We then say that the laminate is subjected to pure shear on its boundary $\partial\mathcal{B}$.

Since the imposed deformation on $\partial\mathcal{B}$ is plane and parallel to the plane defined by the vectors $\{\mathbf{e}_1, \mathbf{e}_2\}$, we expect that the deformation of the laminate is also parallel to this plane and that the vector \mathbf{e}_1 , which defines the direction of lamination in the reference configuration, be mapped into a unit vector $\bar{\mathbf{n}}$ that is parallel to this same plane. The vector $\bar{\mathbf{n}}$ defines a direction of lamination in the deformed configuration and is oriented at an angle ϕ , called *rotation angle of the layers*, with respect to the direction of \mathbf{e}_1 . An illustration of both the reference and the deformed configurations of the laminate under the conditions introduced above is shown in Fig. 2. Using the principal solution for the effective medium, a relation between the vectors \mathbf{e}_1 and $\bar{\mathbf{n}}$ is given by (see, for instance, [10])

$$\bar{\mathbf{n}} = \frac{(\text{cof } \bar{\mathbf{F}}) \mathbf{e}_1}{|(\text{cof } \bar{\mathbf{F}}) \mathbf{e}_1|}. \quad (19)$$

Substituting $\bar{\mathbf{F}}$, given by (18), into (19), we obtain

$$\phi = \arccos \left(\frac{\sqrt{2} (\cos^2 \bar{\Theta} + \bar{\lambda}^2 \sin^2 \bar{\Theta})}{\sqrt{1 + \bar{\lambda}^4 - (\bar{\lambda}^4 - 1) \cos 2\bar{\Theta}}} \right). \quad (20)$$

Observe from (20) that ϕ depends upon $\bar{\Theta}$ and $\bar{\lambda}$ only, being independent of the material properties of the laminate.

We consider a laminate with 256 laminae subject to a state of plane strain parallel to the $X_1 X_2$ -plane and having unit dimensions in planes perpendicular to the X_3 -direction, so that $W \rightarrow \infty$, $C = H = 1$, and $L = 1/256$ in Fig. 1. We also consider that the volume fraction of Phase 1 is $c_1 = 0.7$. We have used ANSYS 10.0 to discretize the laminate with 4096 elements of the type PLANE183², which yields 14345 degrees of freedom. Recall from above that the strain energy function of the compressible Neo-Hookean material that is implemented in ANSYS 10.0 is given

² The element PLANE183 is a two-dimensional, eight-node element with quadratic shape functions for the displacement field, which is well suited to modeling irregular meshes (adapted from ANSYS 10.0 Help Topics).

by (15), where computational results were obtained for $\mu_1 = 1$, $\kappa_1 = 100$, and $\tau = 20$. Thus, the material in Phase 2 is 20 times stiffer than the material in Phase 1.

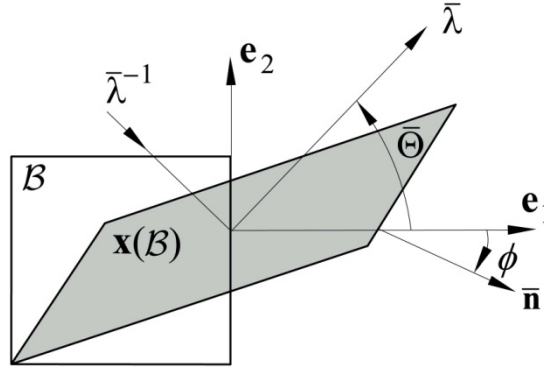


Figure 2: Pure shear of the laminate.

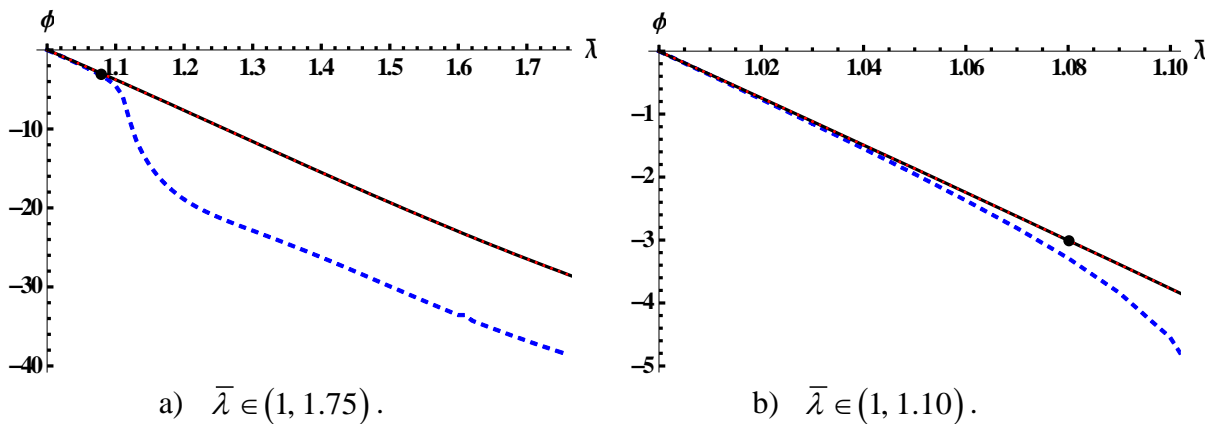
In Fig. 3 we show curves ϕ versus $\bar{\lambda}$ obtained from both the expression (20) with $\bar{\Theta} = 20^\circ$ and from computational results. The graph on the left-hand side of this figure is for $\bar{\lambda} \in (1, 1.75)$ and the graph on the right-hand side corresponds to $\bar{\lambda} \in (1, 1.10)$ in the previous graph. To obtain the computational results, we have evaluated deformation gradients at the centers of two consecutive laminae located at the center of the laminate. Let $\hat{\mathbf{F}}_1$ and $\hat{\mathbf{F}}_2$ be the evaluated gradients at the laminae corresponding to phases 1 and 2, respectively. Substituting the average deformation gradient $\hat{\mathbf{F}} = c_1 \hat{\mathbf{F}}_1 + c_2 \hat{\mathbf{F}}_2$, which is analogous to (12), into (19), we obtain an estimate for the resulting rotation angle of the layers away from the boundary of the bilaminate. In both graphs of Fig. 3, this angle corresponds to the dashed line and the angle ϕ obtained from (20) corresponds to the solid lines. Observe from Fig. 3.a that both curves are indistinguishable for small values of $\bar{\lambda}$, become different for $\bar{\lambda} \cong 1.08$, and then are almost parallel for large values of $\bar{\lambda}$. Observe from Fig. 3.b that the transition from one curve to the other curve is smooth.

In Fig. 3 we also show a dot on the solid line representing the point of the curve where the strong ellipticity condition $(\mathbf{b} \otimes \mathbf{c}) : D^2 \hat{W}(\bar{\mathbf{F}}) [\mathbf{b} \otimes \mathbf{c}] > 0$ for $\mathbf{b}, \mathbf{c} \in \mathbb{R}^3$ fails, where $D^2 \hat{W}(\bar{\mathbf{F}})$ is given by both (13) and (14) and $\hat{W}(\bar{\mathbf{F}})$ is the effective strain energy function given by (11). The dot corresponds to the stretching $\bar{\lambda} \cong 1.08$. Recalling from above that the solid line represents the rotation angle obtained from the principal solution, we then see from Fig. 3 that the dashed line may correspond to a secondary solution, which bifurcates from the principal solution at the point where there is loss of ellipticity for the effective medium.

5 CONCLUSION

We have addressed the equilibrium problem of a two-phase hyperelastic laminate subjected to pure shear on its boundary. Of particular interest here is the case of phases made of compressible Neo-Hookean materials, for which the ellipticity condition (5) holds. Away from the boundary of the laminate, it is possible to obtain a deformation field that is homogeneous in each phase and satisfies appropriate jump conditions at the interface between the phases. This field is used to obtain an average deformation gradient that yields the direction of lamination of the laminate in its

deformed configuration. The average deformation gradient, given by (18) in this work, corresponds to a principal solution of the equilibrium problem for the effective medium. For a moderate value of $\bar{\lambda}$ in (18), the ellipticity condition for this medium fails. To search for a secondary solution that bifurcates from the principal one, we have used FEM to discretize a laminate under a state of plane strain, which is composed of laminae made of the same type of material considered above and subjected to the same state of pure shear on its boundary. We have obtained a deformation gradient field that was used to compute an average deformation gradient, which was then used to obtain an estimate for the rotation angle at the center of the laminate in its deformed configuration. By comparing the rotation angle obtained from the homogenization theory with the one obtained from FEM, we observe that both angles are close to each other for small values of $\bar{\lambda}$ and are very different for large values of $\bar{\lambda}$. The beginning of the transition zone where they become different from each other corresponds to the deformation for which the ellipticity condition for the effective medium fails.

a) $\bar{\lambda} \in (1, 1.75)$.b) $\bar{\lambda} \in (1, 1.10)$.Figure 3: Rotation angle ϕ versus stretching $\bar{\lambda}$.

Solid line: Analytical result from (20). Dashed Line: Computational result.

ACKNOWLEDGEMENTS: Financial support from the Coordination for the Improvement of Higher Education Personnel (CAPES) and the association with the University of Minnesota Supercomputing Institute are gratefully acknowledged.

REFERENCES

- [1] Lopez-Pamies, O.; Ponte Castañeda, P. (2009). "Microstructure Evolution in Hyperelastic Laminates and Implications for Overall Behavior and Macroscopic Stability. *Mechanics of Materials*", 41, 364-374.
- [2] Ponte Castañeda, P., Tiberio, E., 2000. "A second-order homogenization method in finite elasticity and applications to black-filled elastomers". *J. Mech. Phys. Solids* 48, 1389–1411.
- [3] Antman, S.S. (1978). "A Family of Semi-Inverse Problems of Non-Linear Elasticity". In: *Contemporary Developments in Continuum Mechanics and Partial Differential Equations*, G.M. de La Penha & L.A.J. Medeiros, Editors, pp. 1-24, North-Holland, Amsterdam.
- [4] Ciarlet, P.G. (1988). *Mathematical Elasticity - Volume 1: Three-Dimensional Elasticity*.: Elsevier Science Publishers B.V., Amsterdam.

- [5] Knowles, J.K.; Sternberg, E. (1975). "On the Ellipticity of the Equations of Nonlinear Elastostatics for a Special Material". *J. Elasticity*, 5, 341-361.
- [6] Knowles, J.K.; Sternberg, E. (1977). "On the Failure of Ellipticity of the Equations for Finite Elastostatic Plane Strain". *Arch. Rational Mech. Anal.*, 63, 321-336.
- [7] Prado, E.B.T.; Aguiar, A.R. (2009). "Estudo do comportamento de um sólido elástico-linear transversalmente isotrópico via MHA via MEF". *Cadernos de Eng. de Estruturas*, 11, 117-121.
- [8] Pruchnicki, E. (1998). "Hyperelastic law for reinforced elastomer at finite strain with edge effects". *Acta Mech.* 129, 139-162.
- [9] Hill, R. (1972). "On constitutive macro-variables for heterogeneous solids at finite strain". *Proc. R. Soc. Lond. A* 11, 326, 1565, 131-147.
- [10] Gurtin, M.E.; Fried, E.; Anand, L., 2010. *The Mechanics and Thermodynamics of Continua*. Cambridge University Press, Cambridge.